

AD

5009318

TRI-PP-92-127
Dec 1992A study of $\eta \rightarrow \pi^0 \gamma \gamma$ decay using the quark-box diagram

John N. Ng and D.J. Peters

Theory Group, TRIUMF, 4004 Wesbrook Mall, Vancouver, B.C., Canada V6T 2A9

Abstract

We study the decay of η mesons into π^0 and a photon pair via the quark-box mechanism in a phenomenological quark model. The main parameters of the model are the $\eta q q$ and $\pi q q$ couplings, which are fixed by the $\eta \rightarrow \gamma \gamma$ and $\pi^0 \rightarrow \gamma \gamma$ decays. With constituent quark masses of 300 MeV for u - and d -quarks we find the width to be 0.70 eV, in good agreement with the experimental value of 0.84 ± 0.18 eV. In contrast, chiral perturbation theory gives a width of 0.42 eV. Detailed comparison with the vector meson dominance model is also given.



CERN LIBRARIES, GENEVA

CM-P00068351

(submitted to Physical Review D)

I. INTRODUCTION

The radiative decays of light mesons have been a very fertile testing ground of theoretical ideas [1]. In particular, $\pi^0 \rightarrow \gamma \gamma$ decay has led to the triangle anomaly and has profoundly influenced the development of particle physics. Subsequently, many of the radiative decays of the nonet meson were extensively studied, both experimentally and theoretically. The theoretical descriptions fall mainly into two categories: a) chiral perturbation theory where the degrees of freedom used are the low-lying hadron states, and b) quark model descriptions. In chiral perturbation theory (ChPT) [2] the quarks and gluons are integrated out, and hence they do not appear in low-energy effective Lagrangians. On the other hand, the phenomenological quark models make use of constituent quarks in an essential way. By and large, ChPT has been a very successful framework for studying low-energy phenomena. The photon decays of pseudoscalar mesons such as π^0 , η , η' , etc. are described by the Wess-Zumino term, and the Dalitz decays $\pi^0 \rightarrow \gamma e e$, $\eta \rightarrow \gamma e e$, etc. are well explained by vector-meson dominance incorporated into ChPT. The fly in the ointment is the decay

$$\eta \rightarrow \pi^0 \gamma \gamma . \quad (R1)$$

The experimental value for the width [3] of (R1) is

$$\Gamma(\eta \rightarrow \pi^0 \gamma \gamma) = 0.84 \pm 0.18 \text{ eV} . \quad (1.2)$$

In ChPT the decay (R1) occurs at higher order in the momentum (p) expansion, i.e. $O(p^6)$. The most recent calculation in this theory was performed up to $O(p^8)$ and gave the value [4]

$$\Gamma_{\text{ChPT}} = 0.42 \pm 0.20 \text{ eV} . \quad (1.3)$$

Although the order of magnitude is correct, ChPT is about a factor of two smaller than the experimental value when taken seriously.

In a previous paper [5], we used a more phenomenological approach to study (R1) by assuming vector meson dominance (ρ , ω , ϕ) plus the contribution from the a_0 -meson (see Fig. 1). The necessary couplings are determined phenomenologically by the appropriate decays such as $\rho \rightarrow \eta \gamma$, $\pi \gamma$, etc. As expected the dominant contribution comes from the ρ , ω -meson with higher resonances playing lesser roles, and the width in this model is given by

$$\Gamma_{\text{VMD}} = 0.30 \begin{matrix} +0.16 \\ -0.13 \end{matrix} \text{ eV} . \quad (1.4)$$

The a_0 -meson gives at best a 20% correction to the above value. We expect this to be true even when one puts in a myriad of higher meson resonances [6].

In this paper we study (R1) in a constituent quark model framework. We propose that the primary mechanism for (R1) is given by the box diagram of Fig. 2. The use of quark models to study light pseudoscalar decay mesons (P) is not new. It has been applied in $P \rightarrow \gamma \gamma$, $P \rightarrow \ell \bar{\ell}$ and $P \rightarrow \gamma \ell \bar{\ell}$ decays [7]. In these studies it was found that with the correct choice of constituent quark masses the VMD behavior of form factors can be reproduced by the quark loop diagrams. The main parameters of quark models

are the pseudoscalar meson-quark-quark couplings and the constituent quark masses. In our study we shall determine the $\eta q\bar{q}$ and $\pi q\bar{q}$ couplings by fitting the radiative decay widths of $\eta \rightarrow \gamma\gamma$ and $\pi^0 \rightarrow \gamma\gamma$. To simplify the calculation we shall assume that the u - and d -quarks are degenerate in masses, i.e. $m_u = m_d = m$. One can easily generalize to unequal masses. The s -quark mass is fixed at $500 \text{ MeV}/c^2$ since we find that for this problem there is little sensitivity to the s -quark mass. On the other hand, m is allowed to vary within the reasonable range of $280 < m < 330 \text{ MeV}/c^2$.

In Sec. II we outline the calculation of $P \rightarrow \gamma\gamma$ decay and determine the appropriate couplings. The mixing of η - η' is taken into account and the mixing angle of -20° is used [8]. The bulk of the calculation of (R1) using the box diagram is given in Sec. III. We also present double differential cross sections with respect to photon energies as a test to distinguish between different models. It is well known that (R1) is an important input to the calculation of the unitarity lower bound for the decay $\eta \rightarrow \pi\ell\ell$ ($\ell = e, \mu$). This calculation was reported in Ref. [5] with VMD as the dominant mechanism (see also Ref. [9]). In Sec. IV we update the result for the lower bound of both $\eta \rightarrow \pi e\bar{e}$ and $\eta \rightarrow \pi\mu\bar{\mu}$ using the box diagram. Finally, we present our conclusions in Sec. V. An appendix is provided for the reader who wants the mathematical details of the integrals involved in the calculation reported in Sec. III.

II. THE QUARK TRIANGLE AND $P \rightarrow \gamma\gamma$ DECAYS

The main purpose of this section is to set out notation and calculate the couplings $g_{\eta\eta\gamma}$ and $g_{\pi\eta\gamma}$ for use later. Since most of this is well known we shall be brief.

The most general Lorentz and gauge-invariant amplitude for $P \rightarrow \gamma\gamma$ is given by

$$A \equiv H \epsilon_{\mu\nu\rho\sigma} \epsilon_1^\mu \epsilon_2^\nu k_1^\rho k_2^\sigma, \quad (2.1)$$

where M_P is the mass of the decaying meson and k_i , ϵ_i ($i = 1, 2$) are, respectively, the 4-momenta and polarization vectors for the photons, and H is the decay form factor. The width is given by

$$\Gamma(P \rightarrow 2\gamma) = \frac{H^2 M_P^2}{64\pi}. \quad (2.2)$$

In the quark model, H is obtained by calculating the quark triangle diagram. The result for one quark species is

$$H_q = -\frac{2\alpha Q_q^2 g_{Pqq}}{\pi} \frac{m}{M_P^2} \int_0^1 dt \frac{1-2t}{a-t+t^2} \ln(1-t), \quad (2.3)$$

where $a \equiv \frac{m^2}{M_P^2}$. Using Eqs. (2.2),(2.3) and the experimental value of $\pi^0 \rightarrow \gamma\gamma$ width of 7.75 eV , we obtain

$$g_{\pi uu} = g_{\pi dd} = 3.19 \pm 0.11. \quad (2.4)$$

To obtain the $\eta q\bar{q}$ couplings, we have to take into account the η - η' mixing. In the quark model, the η and η' are admixtures of octet and single $q\bar{q}$ states. The physical

states are given by

$$\begin{aligned} \eta &= \frac{\cos\theta}{\sqrt{6}} (\bar{u}u + \bar{d}d - 2s\bar{s}) - \frac{\sin\theta}{\sqrt{3}} (\bar{u}u + \bar{d}d + s\bar{s}) \\ \eta' &= \frac{\sin\theta}{\sqrt{6}} (\bar{u}u + \bar{d}d - 2s\bar{s}) + \frac{\cos\theta}{\sqrt{2}} (\bar{u}u + \bar{d}d + s\bar{s}). \end{aligned} \quad (2.5)$$

The most recent fit [8] gives $\theta = -20^\circ$ and the physical state is given by

$$\eta \simeq 0.58(\bar{u}u + \bar{d}d) - 0.57 s\bar{s}. \quad (2.6)$$

We further assume the couplings of the meson to be independent of flavor, i.e. $g_{\pi uu} = g_{\pi dd} = g_{\pi ss}$, but m_s is taken to be $500 \text{ MeV}/c^2$. This assumption appears to be reasonable and does not contradict any observations. Again using Eqs. (2.2),(2.3) and the experimental value of $\Gamma(\eta \rightarrow \gamma\gamma) = 0.463 \text{ keV}$ [3], we find

$$g_{\eta\eta\gamma} = 1.26 \pm 0.06. \quad (2.7)$$

This completes the determination of the parameters of the model. More detailed values of these couplings for different values of m are given in Table I.

III. THE BOX DIAGRAM

With the determination of $g_{\eta\eta\gamma}$ and $g_{\pi\eta\gamma}$ in the previous section we are now able to calculate the contribution of the quark box diagram to (R1). The decay is governed by the gauge-invariant matrix element given by

$$T = \epsilon_{1\mu} \epsilon_{2\nu} T^{\mu\nu}, \quad (3.1)$$

where [10]

$$\begin{aligned} T^{\mu\nu} &= A(x_1, x_2) \left[k_1^\mu k_2^\nu - k_1 \cdot k_2 g^{\mu\nu} \right] \\ &+ B(x_1, x_2) \left[-M_\eta^2 x_1 x_2 g^{\mu\nu} - \frac{k_1 \cdot k_2}{M_\eta^2} P^\mu P^\nu + x_1 k_2^\mu P^\nu + x_2 P^\mu k_1^\nu \right], \end{aligned} \quad (3.2)$$

where P^μ is the four-momentum of the η meson and M_η denotes its mass. The four-momenta and polarization vectors of the photons are, respectively, given by k_i and ϵ_i ($i = 1, 2$), and $x_i \equiv \frac{P \cdot k_i}{P \cdot k_i}$.

Before we go into the detailed dynamics of A and B , we wish to advocate that the double differential cross section with respect to the photon energies will be a good probe of the physics involved in A and B . To see this explicitly, one examines the differential cross section which is given by

$$\begin{aligned} \frac{d^2\Gamma}{dx_1 dx_2} &= \frac{M_\eta^2}{256\pi^3} \left\{ \left| A + \frac{1}{2} B \right|^2 \left[2(x_1 + x_2) + \frac{M_\eta^2}{M_\eta^2} - 1 \right]^2 \right. \\ &\left. + \frac{1}{4} |B|^2 \left[4x_1 x_2 - \left(2x_1 + 2x_2 - 1 + \frac{M_\eta^2}{M_\eta^2} \right) \right]^2 \right\}. \end{aligned} \quad (3.3)$$

This is general and independent of models for A and B . The Dalitz boundary is given by

$$x_1 + x_2 \geq \frac{M_n^2 - M_\pi^2}{2M_\pi^2} \quad (3.4)$$

and

$$x_1 + x_2 - 2x_1x_2 \leq \frac{M_n^2 - M_\pi^2}{2M_\pi^2}. \quad (3.5)$$

Hence, near the linear part of the Dalitz plot given by Eq. (3.4), a high statistics measurement will be a sensitive test of B .

Next, we turn our attention to the dynamics of the decay which reside in the two form factors A and B and how they behave as functions of x_1 and x_2 . We shall calculate them in the quark model. The set of gauge-invariant one-loop diagrams is given in Fig. 2. Only the u - and d -type quarks contribute since the π^0 does not have any significant $s\bar{s}$ content. The decay structure tensor $T^{\mu\nu}$ is given by a straightforward evaluation of the Feynman diagrams. First we define the quantities $U_i^{\mu\nu}$ ($i = 1, \dots, 6$) by

$$\begin{aligned} T_i^{\mu\nu} &= -3e^2 Q_q^2 g_{qq} g_{\pi q} \int \frac{d^4q}{(2\pi)^4} U_i^{\mu\nu} \\ \text{and } U_1^{\mu\nu} &= \text{Tr} \frac{[\gamma_5(\not{q}+m)\gamma_5(\not{q}+P-k_1-k_2)^2-m^2][(q+P-k_1)^2-m^2][(q+P)^2-m^2]}{(q^2-m^2)((q+P-k_1-k_2)^2-m^2)((q+P-k_1)^2-m^2)((q+P)^2-m^2)}, \\ U_2^{\mu\nu} &= \text{Tr} \frac{[\gamma_5(\not{q}+m)\gamma^\nu(\not{q}+k_2+m)\gamma_5(\not{q}+P-k_1-k_2)^2-m^2][(q+P-k_1)^2-m^2]}{(q^2-m^2)((q+k_2)^2-m^2)((q+P-k_1)^2-m^2)((q+P)^2-m^2)}, \\ U_3^{\mu\nu} &= \text{Tr} \frac{[\gamma_5(\not{q}+m)\gamma^\nu(\not{q}+k_2+m)\gamma^\mu(\not{q}+k_1+k_2)^2-m^2][(q+P)^2-m^2]}{(q^2-m^2)((q+k_2)^2-m^2)((q+k_1+k_2)^2-m^2)((q+P)^2-m^2)}, \\ U_4^{\mu\nu} &= T_1^{\mu\nu}(k_1 \leftrightarrow k_2), \\ U_5^{\mu\nu} &= T_2^{\mu\nu}(k_1 \leftrightarrow k_2), \\ U_6^{\mu\nu} &= T_3^{\mu\nu}(k_1 \leftrightarrow k_2), \end{aligned} \quad (3.6)$$

$$\text{and } T^{\mu\nu} = \sum_{i=1}^6 T_i^{\mu\nu}.$$

Equations (3.6) look prohibitively difficult. However, to extract A and B one needs only to identify the coefficients of $P_\mu P_\nu$ term and $g_{\mu\nu}$ in the structure [see Eq. (3.2)]. This greatly simplifies the calculation, and the rest of the terms can be used as a check. More details of the Feynman integrals are given in Appendix A. In general A and B are complicated functions of x_1 and x_2 which can be written in the form of a double integral. These integrals are complicated Spence functions. To evaluate them analytically will involve hundreds of Spence functions and this we deem to be of dubious value. Instead we evaluated these integrals numerically and fitted A and B by a third degree polynomial function using the routine available in the algebraic

computational program of Ref. [11]. Within the Dalitz region given by Eqs. (3.4) and Eq. (3.5) we find a good fit to A , B is given by

$$\begin{aligned} \frac{Q^2}{M_\pi^2} A(x_1, x_2) &= -0.616 + 2.14(x_1 + x_2) - 2.509(x_1^2 + x_2^2) - 4.184x_1x_2 \\ &+ 1.5896(x_1^3 + x_2^3) + 2.936x_1x_2(x_1 + x_2) \end{aligned} \quad (3.7a)$$

$$\begin{aligned} B(x_1, x_2) &= -0.866 + 1.674(x_1 + x_2) - 3.260(x_1^2 + x_2^2) - 1.781x_1x_2 \\ &+ 2.370(x_1^3 + x_2^3) + 1.089x_1x_2(x_1 + x_2), \end{aligned} \quad (3.7b)$$

where $Q \equiv k_1 + k_2$. The quantities A and B are expressed in units of 10^{-6} MeV $^{-2}$. Expressions (3.7a) and (3.7b) are valid for the value of $m = 300$ MeV/ c^2 quark mass. Since x_1 and x_2 are both small numbers, it is not necessary to go beyond the third degree in the numerical fit. Using the forms of A and B as given by Eq. (3.7a,b) the computer time required to do final phase space integrals over x_1 and x_2 is greatly reduced. Finally, we obtain the width of (R1) in the quark model to be

$$\Gamma(\eta \rightarrow \gamma\gamma\pi^0) = 0.70 \text{ eV} \quad (3.8)$$

for $m = 300$ MeV/ c^2 . In Table I we give the sensitivity of our calculation for a range of reasonable constituent quark masses.

It is interesting that the width given in Eq. (3.8) is close to the experimental value. This is to be compared with the result of the ChPT and VMD model of Eqs. (1.3),(1.4). There are further tests one can use to distinguish between this model and the VMD model. One such test will be the measurement of the dependence of A and B on x_1 and x_2 . In Fig. 3 we showed the difference between the two models for the quantity $\frac{Q^2 A}{M_\pi^2}$ as a function of x_2 for fixed values of x_1 . The box diagram gives a steeper slope than the VMD model. Similar comparisons are given for B , depicted in Fig. 4. For B the x_2 dependences for fixed x_1 are almost indistinguishable between the two models except for the normalization which is larger for the box diagram model.

IV. EFFECTS ON THE UNITARITY BOUND FOR $\eta \rightarrow \pi^0 \ell \bar{\ell}$

In a previous paper we calculated the unitarity bound for the semileptonic decay

$$\eta \rightarrow \pi^0 \mu \bar{\mu} \quad \text{and} \quad \eta \rightarrow \pi^0 e \bar{e} \quad (R2)$$

assuming VMD which gave a low rate for (R1). With the present calculation the unitarity bound is expected to scale up since the rate (R1) is higher for the quark-box mechanism. The unitarity bounds for the decays (R2) are obtained by calculating the imaginary part of the amplitudes, denoted by $\text{Im } A_{27}$, as depicted in Fig. 5 with the two intermediate photons put on-shell. Explicitly, we obtained [5]

$$\text{Im } A_{27} = -\frac{\alpha}{4} \left[ALm\bar{m}\nu + \frac{B}{2} \left(\frac{1}{3\beta^4} (-2 + 20a + 3(1 - 8a + 8a^2)L) \right) \right]$$

$$\begin{aligned}
& 4(P \cdot Q)^2 (1 + 6a + 20a^2 - 6a(1 + 4a^2)L) \\
& + 3sM_n^2 \beta^2 (1 + 26a - 12a(1 + a)L) m_1 \bar{u} v \\
& - \frac{8(P \cdot p_+)(P \cdot p_-)}{3sM_n^2 \beta^6} (1 + 26a - 12a(1 + a)L) m_1 \bar{u} v \\
& + \frac{4P \cdot (p_- - p_+)}{3M_n^2 \beta^4} (1 - a - 3a(1 - 2a)L) \bar{u} p v \Big] , \tag{4.1}
\end{aligned}$$

where

$$\begin{aligned}
a &= \frac{m_1^2}{s} \\
\beta &= \sqrt{1 - 4a} \\
\text{and} \quad L &= \frac{1}{\beta} \ln \frac{1 + \beta}{1 - \beta} . \tag{4.2}
\end{aligned}$$

In general, the A and B form factors have dependence on x_1 and x_2 as calculated in the previous section. We found that it is accurate to approximate them as constant by calculating their average values over the entire physical domain of x_1 and x_2 . This should be an accurate approximation. The unitarity bounds for the widths of (R2) for the quark-box mechanism thus calculated are

$$\Gamma(\eta \rightarrow \pi^0 \mu \bar{\mu}) \Big|_{\text{Box}} \geq 4.3 \pm 0.7 \mu\text{eV} \tag{4.3a}$$

$$\text{and} \quad \Gamma(\eta \rightarrow \pi^0 e \bar{e}) \Big|_{\text{Box}} \geq 2.9 \pm 0.5 \mu\text{eV} \tag{4.3b}$$

for $m = 300 \text{ MeV}/c^2$. Table II displays the results for $280 \leq m \leq 330 \text{ MeV}/c^2$. This is to be compared with the VMD model which are given below [12]

$$\Gamma(\eta \rightarrow \pi^0 \mu \bar{\mu})_{\text{VMD}} \geq 2.4 \pm 0.8 \mu\text{eV} \tag{4.4a}$$

$$\text{and} \quad \Gamma(\eta \rightarrow \pi^0 e \bar{e})_{\text{VMD}} \geq 3.5 \pm 0.8 \mu\text{eV} . \tag{4.4b}$$

It is interesting to note that the $\pi^0 e \bar{e}$ mode is only sensitive to the term involving B . The rest of the amplitude is helicity suppressed. On the other hand, the $\pi^0 \mu \bar{\mu}$ mode involves interference between A and B and hence is more sensitive to the dynamics involved. This interference is sufficient to overcome the phase space suppression [12] and we obtain $\Gamma(\pi^0 \mu \bar{\mu}) > \Gamma(\pi^0 e \bar{e})$. With these enhancements, the measurements of these semileptonic decays should be within reach of the proposed “ η -factories” [13].

V. CONCLUSIONS

We have studied the decay (R1) within the context of a naïve quark model. The model is predictive with regard to this decay and gives a value of the decay width in agreement with the current experimental value. The calculation using VMD is about a factor of two lower than experiment. Interestingly, if one replaces the quark in our model by a nucleon (N) loop and the couplings by πNN and ηNN , the contribution is an order of magnitude too small to account for the data. This arises from the fact the structure form factors A and B behave as $\frac{1}{M^4}$ for large M , where M is the mass of the fermion in the loop. Replacing quark masses by nucleon mass suppresses A and B by two orders of magnitude. On the other hand, πNN and ηNN couplings are larger than their quark counterparts by only an order of magnitude. As a result, the nucleon box diagram is not important for (R1).

Although our calculation gives a larger branching ratio than ChPT, given the uncertainties involved they should be interpreted as being consistent with each other. This is seen by examining Table I. Since the experiments involved are very difficult and the statistics are not high, one cannot definitely say that ChPT and VMD models are disfavored by experiments. However, a persistent high value for the rate of (R1) would be difficult to accommodate in ChPT/VMD models. We cannot overemphasize the importance of precision measurement of (R1) in future experiments.

We have also examined the model dependence of the form factors A and B . In order to be able to distinguish between models one needs to measure the x_1 and x_2 dependence of these quantities. In particular, the form factor A has different behaviors in x_1 and x_2 for the quark model versus the VMD model. On the other hand, the difference is small for the form factor B , other than overall normalization. These studies would require high statistics measurements. These can certainly be performed at η -factory investigations. In our view, a study of the decay $\eta \rightarrow \pi \gamma \gamma$ will add invaluable to our understanding of low-energy hadron dynamics and will be an important test of chiral perturbation theory as well as the concept of duality in hadron physics.

This research is supported partially by the Natural Sciences and Engineering Research Council of Canada.

Appendix

Appendix A

In this appendix we show some of the mathematical details involved in extracting the form factors A and B from Eqs. (3.6). As has already been mentioned, we need to find only the coefficients of $g^{\mu\nu}$ and $P^\mu P^\nu$, since they are related in a simple way to the form factors. Therefore, in calculating the traces in (3.6), we need only keep the $g^{\mu\nu}$, $P^\mu P^\nu$, $P^\mu q^\nu$, $q^\mu P^\nu$, and $q^\mu q^\nu$ terms. Arranging these terms so as to provide as much cancellation with the denominators as possible, one finds

$$\begin{aligned}
 U_1^{\mu\nu} = & -4 \left\{ g^{\mu\nu} \left[\frac{1}{2} D_2^{-1}(0, P-k_1) + \frac{1}{2} D_2^{-1}(0, -Q) + \frac{1}{4} (2P \cdot k_2 - Q^2) D_3^{-1}(0, P-Q, P-k_1) \right. \right. \\
 & + \frac{1}{2} (P \cdot Q - P^2) D_3^{-1}(0, P-Q, P) - \frac{1}{2} P \cdot k_1 D_3^{-1}(0, P-k_1, P) \\
 & + \frac{1}{4} Q^2 D_3^{-1}(0, -Q, -k_1) + \frac{1}{4} Q^2 (2P \cdot k_1 - P^2) D_4^{-1}(0, P-Q, P-k_1, P) \left. \right\} \\
 & + q^\mu q^\nu \left[-2D_3^{-1}(0, -Q, -k_1) + 2(P^2 - P \cdot Q) D_4^{-1}(0, P-Q, P-k_1, P) \right] \\
 & + \frac{1}{2} (P^\mu q^\nu + q^\mu P^\nu) \left[-D_3^{-1}(0, P-Q, P-k_1) - D_3^{-1}(0, P-k_1, P) \right. \\
 & + (Q^2 + 4P^2 - 4P \cdot Q) D_4^{-1}(0, P-Q, P-k_1, P) \left. \right] \\
 & + P^\mu P^\nu \left[-D_3^{-1}(0, P-Q, P-k_1) - D_3^{-1}(0, P-k_1, P) \right. \\
 & + (2P^2 - 2P \cdot Q + Q^2) D_4^{-1}(0, P-Q, P-k_1, P) \left. \right\} + \dots \\
 U_2^{\mu\nu} = & -4 \left(g^{\mu\nu} \left[-\frac{1}{2} D_2^{-1}(0, P-k_1) - \frac{1}{2} D_2^{-1}(0, P-k_2) + \frac{1}{4} (Q^2 - 2P \cdot k_2) D_3^{-1}(0, k_2, P-k_1) \right. \right. \\
 & + \frac{1}{2} P \cdot k_2 D_3^{-1}(0, P, k_2) + \frac{1}{2} P \cdot k_1 D_3^{-1}(0, P-k_1, P) \\
 & + \frac{1}{4} (Q^2 - 2P \cdot k_1) D_3^{-1}(0, P-Q, P-k_2) + \frac{1}{4} (4P \cdot k_1 \cdot P \cdot k_2 - P^2 Q^2) D_4^{-1}(0, k_2, P-k_1, P) \left. \right] \\
 & + 2q^\mu q^\nu (P^2 - P \cdot Q) D_4^{-1}(0, k_2, P-k_1, P) \\
 & + \frac{1}{2} (P^\mu q^\nu + q^\mu P^\nu) \left[-D_3^{-1}(0, k_2, P-k_1) - D_3^{-1}(0, k_2, P) + D_3^{-1}(0, P-k_1, P) \right. \\
 & + D_3^{-1}(0, P-Q, P-k_2) + 2(P^2 - P \cdot Q) D_4^{-1}(0, k_2, P-k_1, P) \left. \right] \\
 & + P^\mu P^\nu \left[D_3^{-1}(0, P-k_1, P) + D_3^{-1}(0, P-Q, P-k_2) \right] + \dots \\
 U_3^{\mu\nu} = & -4 \left(g^{\mu\nu} \left[\frac{1}{2} D_2^{-1}(0, Q) + \frac{1}{2} D_2^{-1}(0, P-k_2) + \frac{1}{4} Q^2 D_3^{-1}(0, k_2, Q) - \frac{1}{2} P \cdot k_2 D_3^{-1}(0, k_2, P) \right. \right. \\
 & + \frac{1}{2} (P \cdot Q - P^2) D_3^{-1}(0, Q, P) + \frac{1}{4} (2P \cdot k_1 - Q^2) D_3^{-1}(0, k_1, P-k_2) \\
 & + \frac{1}{4} (2P \cdot k_2 - P^2) Q^2 D_4^{-1}(0, k_2, Q, P) \left. \right] \\
 & + q^\mu q^\nu \left[-2D_3^{-1}(0, k_2, Q) + 2(P^2 - P \cdot Q) D_4^{-1}(0, k_2, Q, P) \right] \\
 & + \frac{1}{2} (q^\mu P^\nu + P^\mu q^\nu) \left[D_3^{-1}(0, k_2, P) + D_3^{-1}(0, k_1, P-k_2) - Q^2 D_4^{-1}(0, k_2, Q, P) \right] + \dots, \tag{A.1}
 \end{aligned}$$

where

$$D_n(p_1, \dots, p_n) = \prod_{i=1}^n ((q+p_i)^2 - m^2) \tag{A.2}$$

and m is the quark mass. By “+...” we mean terms which do not, after integration, contribute to the $g^{\mu\nu}$ and $P^\mu P^\nu$ terms in $T^{\mu\nu}$. In order to make the integrals simpler, we have used the substitutions $q \rightarrow q-P$, $q \rightarrow q-k_1$, $q \rightarrow q-k_2$, to ensure that each denominator contains one factor of $q^2 - m^2$.

Some of the integrals in $T^{\mu\nu}$ are divergent. We handle this by the standard dimensional regularization method, where the number of space time dimensions is $n = 4 - \epsilon$. We define

$$\Delta \equiv \frac{i}{16\pi^2} \left(\frac{2}{\epsilon} - 7E + \epsilon n 4\pi \right), \tag{A.3}$$

where $7E$ is Euler's constant. The only kinds of integrals in $T^{\mu\nu}$ which are divergent are

$$\begin{aligned}
 & \int \frac{d^n q}{(2\pi)^n} D_2^{-1}(a, 0) = \Delta + O(1), \quad \text{and} \\
 & \int \frac{d^n q}{(2\pi)^n} q^\mu q^\nu D_3^{-1}(a, b, 0) = \frac{1}{4} g^{\mu\nu} \Delta + O(1) \tag{A.4}
 \end{aligned}$$

so we can easily identify the divergences arising from integrating (A.1). The divergences all reside in the coefficients of $g^{\mu\nu}$ term and they cancel as expected leaving only a finite piece.

For the sake of keeping the integrated expressions short, we define the following quantities

$$\begin{aligned}
 I(a) & \equiv \lim_{\epsilon \rightarrow 0} \left(-\Delta + \int \frac{d^n q}{(2\pi)^n} D_2^{-1}(a, 0) \right) = -\frac{i}{16\pi^2} \int_0^1 dx \ln(m^2 - a^2 x(1-x)) \\
 J(a, b) & \equiv \int \frac{d^4 q}{(2\pi)^4} D_3^{-1}(a, b, 0) = -\frac{i}{16\pi^2} \int_0^1 dx \int_0^{1-x} dy \\
 & \quad \times (m^2 - a^2 x(1-x) - b^2 y(1-y) + 2a \cdot bxy)^{-1} \\
 J^\mu(a, b) & \equiv \int \frac{d^4 q}{(2\pi)^4} q^\mu D_3^{-1}(a, b, 0) = \frac{i}{16\pi^2} \int_0^1 dx \int_0^{1-x} dy (a^\mu x + b^\mu y) \\
 & \quad \times (m^2 - a^2 x(1-x) - b^2 y(1-y) + 2a \cdot bxy)^{-1} \\
 J^{\mu\nu}(a, b) & \equiv \lim_{\epsilon \rightarrow 0} \left(-\frac{1}{4} g^{\mu\nu} \Delta + \int \frac{d^n q}{(2\pi)^n} q^\mu q^\nu D_3^{-1}(a, b, 0) \right) = -\frac{i}{16\pi^2} \int_0^1 dx \int_0^{1-x} dy \left[(a^\mu x + b^\mu y) \right. \\
 & \quad \left. + \frac{1}{2} g^{\mu\nu} \ln(m^2 - a^2 x(1-x) - b^2 y(1-y) + 2a \cdot bxy) \right] \\
 K(a, b, c) & \equiv \int \frac{d^4 q}{(2\pi)^4} D_4^{-1}(a, b, c, 0) = \frac{i}{16\pi^2} \int_0^1 dx \int_0^{1-x} dy \int_0^{1-x-y} dz (m^2 - a^2 x(1-x) \\
 & \quad - b^2 y(1-y) - c^2 z(1-z) + 2a \cdot bxy + 2a \cdot czx + 2b \cdot cyz)^{-2} \\
 K^\mu(a, b, c) & \equiv \int \frac{d^4 q}{(2\pi)^4} q^\mu D_4^{-1}(a, b, c, 0) = -\frac{i}{16\pi^2} \int_0^1 dx \int_0^{1-x} dy \int_0^{1-x-y} dz (a^\mu x + b^\mu y + c^\mu z) \\
 & \quad \times (m^2 - a^2 x(1-x) - b^2 y(1-y) - c^2 z(1-z) + 2a \cdot bxy + 2a \cdot czx + 2b \cdot cyz)^{-2} \\
 K^{\mu\nu}(a, b, c) & \equiv \int \frac{d^4 q}{(2\pi)^4} q^\mu q^\nu D_4^{-1}(a, b, c, 0) = \frac{i}{16\pi^2} \int_0^1 dx \int_0^{1-x} dy \int_0^{1-x-y} dz \left[(a^\mu x + b^\mu y + c^\mu z) \right. \\
 & \quad \left. \times (a^\nu x + b^\nu y + c^\nu z) (m^2 - a^2 x(1-x) - b^2 y(1-y) - c^2 z(1-z) \right. \\
 & \quad \left. + 2a \cdot bxy + 2a \cdot czx + 2b \cdot cyz)^{-2} - \frac{1}{2} g^{\mu\nu} (m^2 - a^2 x(1-x) - b^2 y(1-y) \right. \\
 & \quad \left. - c^2 z(1-z) + 2a \cdot bxy + 2a \cdot czx + 2b \cdot cyz)^{-1} \right]. \tag{A.5}
 \end{aligned}$$

We also define the functions $J_{(i)}$, \tilde{J} , \hat{J} , \bar{J} by

$$\begin{aligned} J^\mu(a_1, a_2) &= -\sum_i a_i^\mu J_{(i)}(a_1, a_2) \\ \hat{J}(a_1, a_2) &= \sum_i J_{(i)}(a_1, a_2) \\ J^{\mu\nu}(a_1, a_2) &= \sum_{i,j} a_i^\mu a_j^\nu J_{(ij)}(a_1, a_2) + g^{\mu\nu} \bar{J}(a_1, a_2) \\ \bar{J}(a_1, a_2) &= \sum_{i,j} J_{(ij)}(a_1, a_2), \end{aligned} \quad (\text{A.6})$$

where the sums all go from 1 to 2. $K_{(i)}$, \widehat{K} , \bar{K} , and \widehat{K} are defined similarly, but they have three arguments so their sums go from 1 to 3.

If we call $V^{\mu\nu}$ the finite contributions to the $g^{\mu\nu}$ and $P^\mu P^\nu$ terms in the integrals of $U_i^{\mu\nu}$, and define \mathcal{A} and \mathcal{B} by

$$\sum_{i=1}^6 V_i^{\mu\nu} = \mathcal{A} g^{\mu\nu} + \mathcal{B} P^\mu P^\nu / M_n^2. \quad (\text{A.7})$$

then comparing (A.1) to the definitions (A.5) and (A.6) gives, after a bit of algebra,

$$\begin{aligned} \mathcal{A} &= -4 \left[2I(Q) + \frac{1}{2} Q^2 (J(k_1, Q) + J(k_2, Q)) \right] + (P \cdot Q - P^2) (J(P, Q) + J(P, P - Q)) \\ &\quad + \frac{1}{4} Q^2 (2P \cdot k_1 - P^2) (K(P, P - k_1, P - Q) + K(P, k_1, Q)) \\ &\quad + \frac{1}{4} Q^2 (2P \cdot k_2 - P^2) (K(P, P - k_2, P - Q) + K(P, k_2, Q)) \\ &\quad + \frac{1}{2} (4P \cdot k_1 P \cdot k_2 - P^2 Q^2) (K(P, k_1, P - k_2) + K(P, k_2, P - k_1)) \\ &\quad - 4(\hat{J}(k_1, Q) + \bar{J}(k_2, Q)) \\ &\quad 2(P^2 - P \cdot Q) (\widehat{K}(P, P - k_1, P - Q) + \widehat{K}(P, P - k_2, P - Q) + \widehat{K}(P, k_2, P - k_1) \\ &\quad + \widehat{K}(P, k_1, Q) + \widehat{K}(P, k_2, Q)) \end{aligned} \quad (\text{A.8})$$

and

$$\begin{aligned} \mathcal{B} &= -4M_n^2 \left[(2P^2 - 2P \cdot Q + Q^2) (K(P, P - k_1, P - Q) + K(P, P - k_2, P - Q)) \right. \\ &\quad + 2(P^2 - P \cdot Q) \left[-\sum_{i=2}^3 (K_{(i)}(k_1, P, P - k_2) + K_{(i)}(k_2, P, P - k_1)) \right. \\ &\quad \left. + \sum_{i=2}^3 \sum_{j=2}^3 (K_{(ij)}(k_1, P, P - k_2) + K_{(ij)}(k_2, P, P - k_1)) \right. \\ &\quad \left. + \widehat{K}(P, P - k_1, P - Q) + \widehat{K}(P, P - k_2, P - Q) + K_{(33)}(k_1, Q, P) + K_{(33)}(k_2, Q, P) \right] \\ &\quad - (4P^2 - 4P \cdot Q + Q^2) (\widehat{K}(P, P - k_1, P - Q) + \widehat{K}(P, P - k_2, P - Q)) \\ &\quad + Q^2 (K_{(3)}(k_1, Q, P) + K_{(3)}(k_2, Q, P)) \end{aligned} \quad (\text{A.9})$$

We wish to write \mathcal{A} and \mathcal{B} as integrals of Feynman parameters, as in (A.5). It is easy to perform the first Feynman parameter integration in the cases where one of the 4-vectors in the expression is null. By using

$$\begin{aligned} K(P, P - k_i, P - Q) &= K(P, k_i, Q) \\ \widehat{K}(P, P - k_i, P - Q) &= -K_{(i)}(P, k_i, Q) + K(P, k_i, Q) \\ \widehat{\widehat{K}}(P, P - k_i, P - Q) &= K_{(ii)}(P, k_i, Q) - 2K_{(i)}(P, k_i, Q) + K(P, k_i, Q) \\ \bar{K}(P, P - k_i, P - Q) &= \bar{K}(P, k_i, Q) \end{aligned} \quad (\text{A.10})$$

We can ensure that k_1 or k_2 appears as an argument in every K -type function. We get

$$\begin{aligned} \mathcal{A} &= \frac{i}{4\pi^2} \left[2 - \left(1 - \frac{4\rho}{\sigma}\right) \int_0^1 \frac{dx}{x} \ln \left(1 - \frac{\sigma}{\rho} x(1-x)\right) \right. \\ &\quad \left. + \int_0^1 dx \int_0^{1-x} dy \left\{ \frac{1}{\rho - x(1-x) - \sigma y(1-y) + 2(1-x_1-x_2)xy} + \frac{\frac{1}{2}\sigma(1-2x_1)}{2x_1x + \sigma y} \right. \right. \\ &\quad \left. \times \left(\frac{1}{\rho - x(1-x) - \sigma y(1-y) + 2(x_1+x_2)xy} - \frac{\rho - x(1-x) + (1-\alpha)xy + 2x_1x(1-x-y)}{1} \right) \right. \\ &\quad \left. + (x_1 \leftrightarrow x_2) + \frac{\frac{1}{2}\sigma - x_1x_2}{2x_1x + (1-\alpha-2x_2)y} \left(\frac{\rho - x(1-x-y) - (1-2x_2)y(1-x-y)}{1} \right) \right. \\ &\quad \left. - \frac{\rho - \alpha y(1-x-y) - (1-2x_1)x(1-x-y)}{1} \right) + (x_1 \leftrightarrow x_2) \\ &\quad + 2(1-x_1-x_2) \ln \left(\frac{\rho - \alpha(1-x) + (1-\alpha)xy + 2x_1x(1-x-y)}{\rho - x(1-x) - \sigma y(1-y) + 2(x_1+x_2)xy} \right) + (x_1 \leftrightarrow x_2) \\ &\quad \left. + \frac{1-x_1-x_2}{2x_1x + (1-\alpha-2x_2)y} \ln \left(\frac{\rho - \alpha y(1-x-y) - (1-2x_1)x(1-x-y)}{\rho - x(1-x-y) - (1-2x_2)y(1-x-y)} \right) + (x_1 \leftrightarrow x_2) \right\} \end{aligned} \quad (\text{A.11})$$

and

$$\begin{aligned} \mathcal{B} &= \frac{i}{4\pi^2} \int_0^1 dx \int_0^{1-x} dy \left[\frac{2\sigma x + 4(1-x_1-x_2)x^2}{2x_1x + \sigma y} \left(\frac{1}{\rho - x(1-x) - \sigma y(1-y) + 2(x_1+x_2)xy} \right. \right. \\ &\quad \left. \left. - \frac{1}{\rho - x(1-x) + (1-\alpha)xy + 2x_1x(1-x-y)} \right) + (x_1 \leftrightarrow x_2) \right. \\ &\quad \left. + \frac{2(1-x_1-x_2)(x+y)(1-x-y)}{2x_1y + (1-\alpha-2x_2)x} \left(\frac{1}{\rho - (1-2x_2)x(1-x-y) - y(1-x-y)} \right. \right. \\ &\quad \left. \left. - \frac{1}{\rho - (1-2x_1)y(1-x-y) - \alpha x(1-x-y)} \right) + (x_1 \leftrightarrow x_2) \right], \end{aligned} \quad (\text{A.12})$$

where $a = \frac{M_n^2}{M_n^2}$, $\rho = \frac{m^2}{M_n^2}$, and $\sigma = \frac{Q^2}{M_n^2} = -(1-\alpha-2(x_1+x_2))$. These are the double integrals referred to in the discussion after Eqs. (3.6).

From (3.2), (3.6), (A.7) and the definition of $V_i^{\mu\nu}$ one sees that

$$\mathcal{A} = -\sum_q 3e^2 Q_q^2 g_{\text{res}} g_{\text{res}} \left(-\frac{1}{k_1 \cdot k_2} \mathcal{A} + \frac{M_n^2 x_1 x_2}{(k_1 \cdot k_2)^2} \mathcal{B} \right) \quad \text{and}$$

$$B = - \sum_q 3e^2 Q_q^2 g_{\eta qq} g_{\pi qq} \left(-\frac{1}{k_1 \cdot k_2} B \right), \quad (\text{A.13})$$

where the sum is over the quark flavours and A and B are given by (A.11) and (A.12).

Table I. The effect of varying the constituent quark mass m on $g_{\pi qq}$, $g_{\eta qq}$ and the width Γ of η to $\pi^0 \gamma \gamma$ decay.

m (MeV/c ²)	$g_{\eta qq}$	$g_{\pi qq}$	$\Gamma(\eta \rightarrow \pi^0 \gamma \gamma)$ (eV)
280	0.95 ± 0.04	2.96 ± 0.11	0.97 ± 0.16
300	1.26 ± 0.06	3.19 ± 0.11	0.70 ± 0.12
330	1.62 ± 0.07	3.52 ± 0.13	0.60 ± 0.10

Table II. The width of $\eta \rightarrow \pi^0 \mu \bar{\mu}$ and $\pi^0 e \bar{e}$ by virtue of the quark-box mechanism for u, d -quarks in the range 280 to 330 MeV/c².

m	$\Gamma(\eta \rightarrow \pi^0 e \bar{e})$ (μeV)	$\Gamma(\eta \rightarrow \pi^0 \mu \bar{\mu})$ (μeV)
280	7.3 ± 1.2	3.9 ± 0.7
300	2.9 ± 0.5	4.3 ± 0.7
330	1.2 ± 0.2	4.3 ± 0.7

Figure captions

1. The radiative decay $\eta \rightarrow \pi^0 \eta \gamma$. Vector meson dominance (VMD) model is depicted in (a) and a_0 -meson mechanism is given in (b).
2. The quark-box diagram mechanism for the decay $\eta \rightarrow \pi^0 \gamma \gamma$.
3. Dependence of the form factor A_1^2 on x_2 for fixed values of x_1 . The solid line is for quark box mechanism and the dash line denotes VMD.
4. The dependence of the form factor $-B$ on x_2 for fixed values of x_1 . The solid line is for quark box mechanism and the dash line denotes VMD.
5. The decay of $\eta \rightarrow \pi \ell \bar{\ell}$ ($\ell = e$ or μ) via the two-photon intermediate state.

References

- [1] For a recent review of light hadron physics, see L.G. Lansberg, *Sov. Phys. Usp.* **35**, 1 (1992).
- [2] J. Gasser and H. Leutwyler, *Nucl. Phys.* **B250**, 465 and 539 (1985).
- [3] Particle Data Group, *Phys. Rev. D* **45**, S1 (1992).
- [4] Ll. Ametller, J. Bijnens, A. Bramon, and F. Cornet, *Phys. Lett. B* **276**, 185 (1992).
- [5] J.N. Ng and D.J. Peters, *Phys. Rev. D* **46** (in press); earlier work includes S. Oneda and G. Oppo, *ibid.* **160**, 1397 (1967); A. Baracca and A. Bramon, *Nuovo Cimento* **69A**, 613 (1970).
- [6] Independently, the authors of Ref. [5] also considered the effects of extra meson contributions. Unless there exist higher meson resonances with unexpectedly large couplings to $\eta \gamma$ or $\pi \gamma$, their contribution to (R1) will be proportional to M^{-4} for heavy meson resonances of mass M .
- [7] R. Van Royon and V.F. Weisskopf, *Nuovo Cimento* **50A**, 617 (1967); L. Bergstrom, *Z. Phys. C* **14**, 129 (1982); C. Hayne and N. Isgur, *Phys. Rev D* **25**, 1944 (1982); Z.P. Li, F.E. Close, and T. Barnes, *ibid.*, **43**, 2161 (1991);
- [8] Ll. Ametller, L. Bergstrom, A. Bramon, and E. Masso, *Nucl. Phys.* **B228**, 301 (1987); B. Margolis, J.N. Ng, M. Phipps, and M.D. Trotter, (to be published in *Phys. Rev. D* (1993)).
- [9] F.J. Gilman and R. Kaufman, *Phys. Rev. D* **36**, 2761 (1987); Most recent experimental determination from the Crystal Barrel Collaboration gives $\theta = -(17.3 \pm 1.8)^\circ$. See C. Anisler *et al.*, *Phys. Lett. B* **294**, 451 (1992).
- [10] T.P. Cheng, *Phys. Rev.* **162**, 1734 (1967); C. Llewellyn-Smith, *Nuovo Cimento* **A3**, 834 (1967).
- [11] G. Ecker, A. Pich, and E. de Rafael, *Nucl. Phys.* **B303**, 665 (1988).
- [12] S. Wolfram, *Mathematica*, 2nd Edition (Addison-Wesley, Redwood City, CA, 1991).
- [13] The values given here differ from that of ref. 5. We have used a more accurate approximation for A and B . We performed a Taylor expansion of A and B and kept terms linear in M^2 , x_1 and x_2 . Previously, these terms were neglected and they make a difference in the unitarity bounds for R2 especially for the $\pi^0 \mu \bar{\mu}$ mode.
- [14] For a review of the η -factory project, see B. Mayer, in *Proceedings of Rare Decays of Light Mesons*, edited by B. Mayer (Frontières, Gif-sur-Yvette, 1990), p. 199.

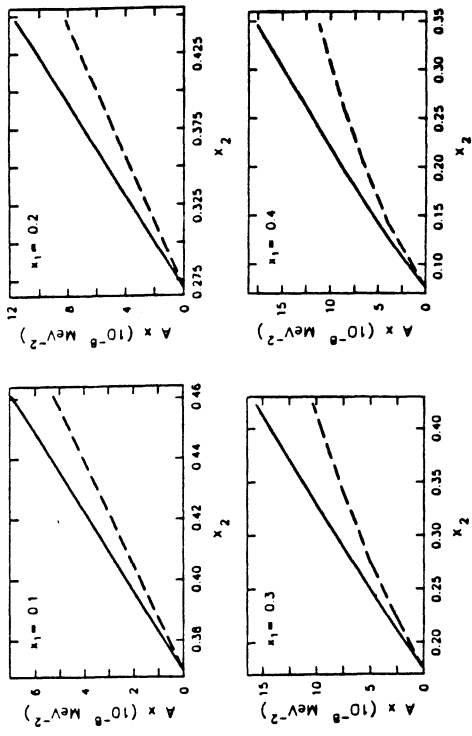
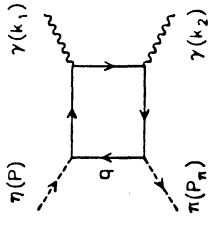
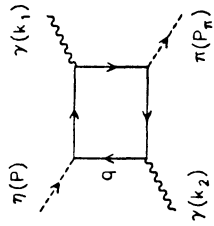
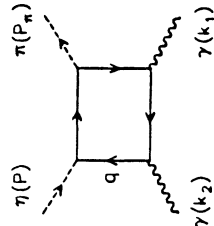


Fig. 3



+ (k_1 ↔ k_2)

Fig. 2

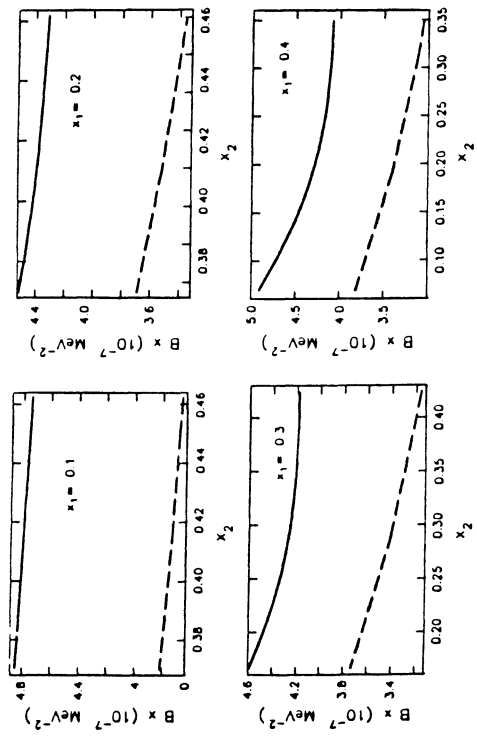
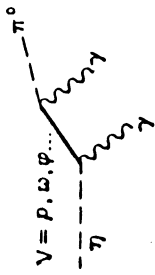
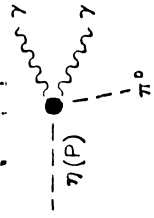


Fig. 4



(a)

(b)

Fig. 1

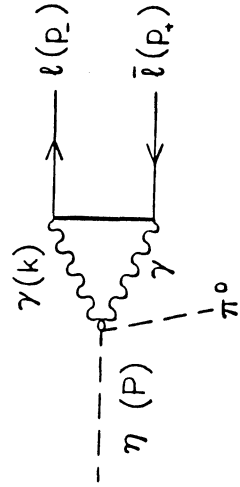


Fig. 5